

Supporting Information

Highly nitrogen-doped mesoscopic carbons as efficient metal-free electrocatalysts for oxygen reduction reactions

Chin-Te Hung,^{a,#} Ningya Yu,^{b,#} Chia-Ting Chen,^{a,c} Pei-Hao Wu,^a Xiaoxiang Han,^d Yu-Siang Kao,^{a,e} Tuan-Chi Liu,^e Feng Deng,^f Anmin Zheng^{f,*} and Shang-Bin Liu^{a,b,*}

^a*Institute of Atomic and Molecular Sciences, Academia Sinica, Taipei 10617, Taiwan,*

^b*Key Lab of Sustainable Resources Processing and Advanced Materials of Hunan Province, Hunan Normal University, Changsha 410081, China*

^c*Department of Chemistry, National Taiwan Normal University, Taipei 11677, Taiwan*

^d*Department of Applied Chemistry, Zhejiang Gongshang University, Hangzhou, 310035, China*

^e*Department of Chemical Engineering, National Taiwan University of Science and Technology, Taipei 10607, Taiwan*

^f*State Key Laboratory of Magnetic Resonance and Atomic and Molecular Physics, Wuhan Institute of Physics and Mathematics, Chinese Academy of Sciences, Wuhan 430071, China.*

***Corresponding authors:**

E-mail: sbliu@sinica.edu.tw (SBL)

E-mail: zhenganm@wipm.ac.cn (AZ)

[#]These authors contributed equally.

Table S1 HOMO-LUMO energy gap, spin density, and charge density of pure and N-doped graphene structures.

Type	Energy (eV)			Maximum spin density*	Maximum charge density*
	HOMO	LUMO	Gap		
Graphene (G)	-9.54	-6.65	2.89	0 (0%)	0.056 (~ 0%)
Pyrrolic-N (N5)	-8.50	-6.11	2.39	0.669 (4.8%)	0.168 (9.5%)
Pyridinic-N (N6)	-8.32	-6.24	2.08	0.290 (27.8%)	0.178 (11.1%)
Quaternary-N (NQ)	-6.81	-6.59	0.22	0.315 (13.0%)	0.223 (13.0%)
Pyridinic-N ⁺ -O ⁻ (NX)	-7.64	-6.27	1.37	0.192 (22.2%)	0.155 (11.1%)

* In unit of $|e|$. The values in parenthesis represent percentage of atoms with a spin or charge density greater than $0.15 |e|$ divided by the total number of atoms in the graphene structure (excluding H and N atoms).

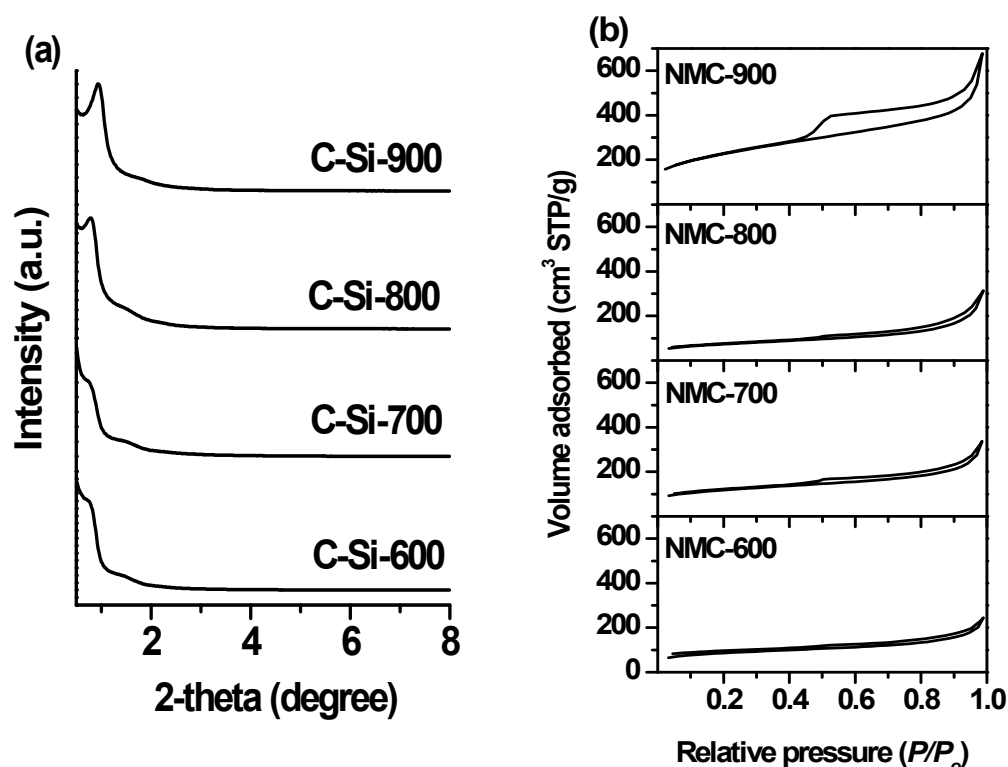


Fig. S1 (a) Small-angle XRD patterns of N-doped C-Si-T composites and (b) N₂ adsorption/desorption isotherms of NMC-T samples prepared with different carbonization temperatures (T = 600, 700, 800, and 900 °C) under microwave irradiation.

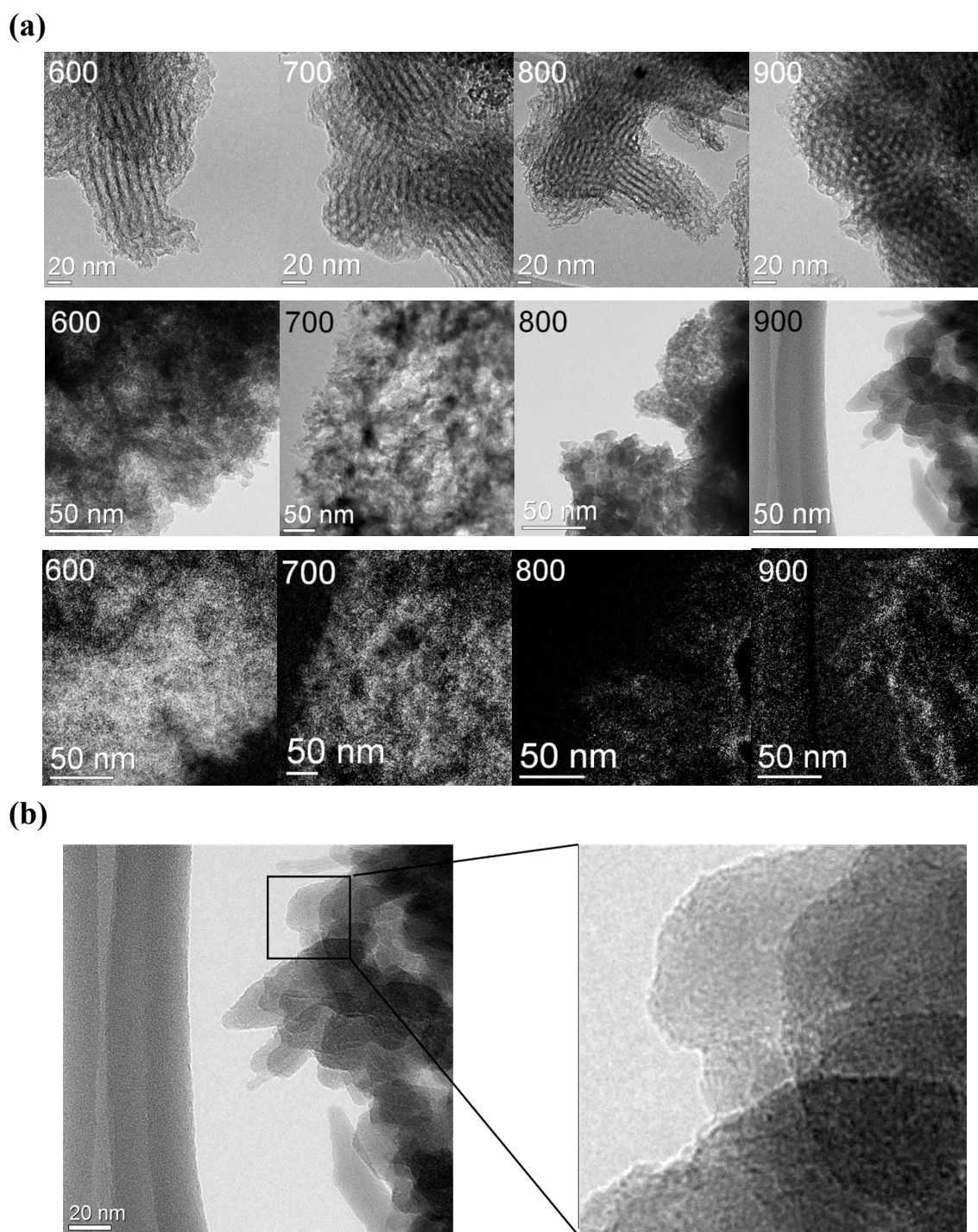


Fig. S2 (a) TEM images of various C-Si-T (Top) and NMC-T (middle) materials with varied carbonization temperature T ranging from 600 to 900 °C. Bottom: EELS N-mapping images of NMC-Ts, and (b) enlarged TEM image of NMC-900

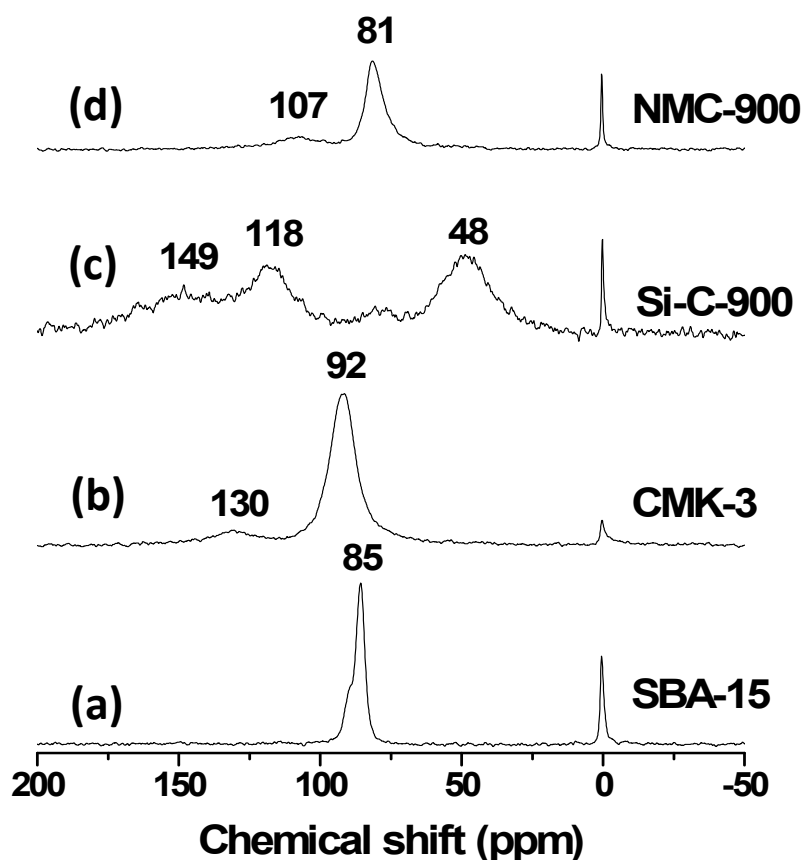


Fig. S3 Room-temperature ^{129}Xe NMR spectra of (a) ordered mesoporous silica SBA-15 and (b) its carbon replica (CMK-3). (c) C-Si-900, and (d) NMC-900. All spectra were recorded with a fixed xenon loading (equilibrium pressure 760 Torr) and same number of scans (NS) of 8,000 except for the Si-C-900, which was acquired with NS = 16,000. Similar to SBA-15 and CMK-3 with ordered mesostructures, the NMC-900 also shows existence of mesoporosities, as revealed by the peak at a ^{129}Xe chemical shift (δ) of ca. 81 ppm. Additional peak at $\delta \sim 107$ ppm may be attributed to the presence of micropores. On the other hand, no mesoporosity was found for the Si-C-900 (before silica template removal); the substrate show only micropores ($\delta \sim 118$ and 149 ppm) and very large pore ($\delta \sim 48$ ppm); the latter is most likely arising from inter-particle voids.

Experimental details: all spectra were recorded on a Bruker-Biospin Avance-300 spectrometer operating at a Larmor frequency of 83.02 MHz using a single-pulse sequence with pulse-width of 3 μs and recycle delay of 2 s. The ^{129}Xe chemical shift was referred to that of dilute Xe gas (0 ppm).

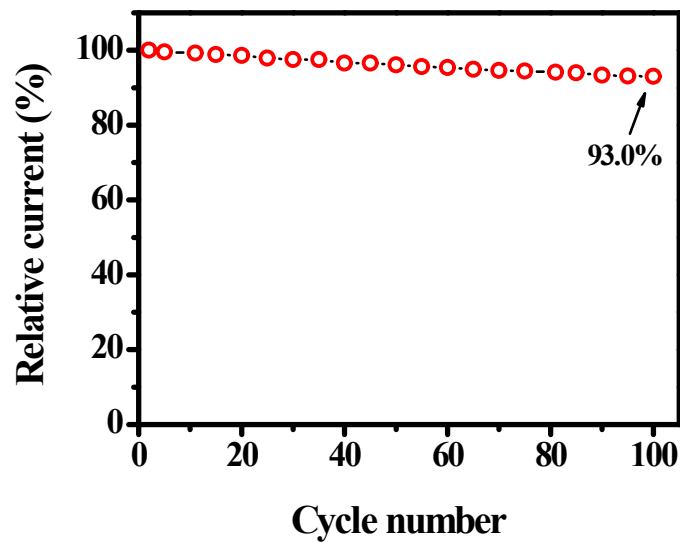


Fig. S4 Durability of NMC-900 up to 100 CV cycles. Only assorted results are shown for clarity reason. Relative currents were calculated based on oxygen reduction peak at -0.26 V.

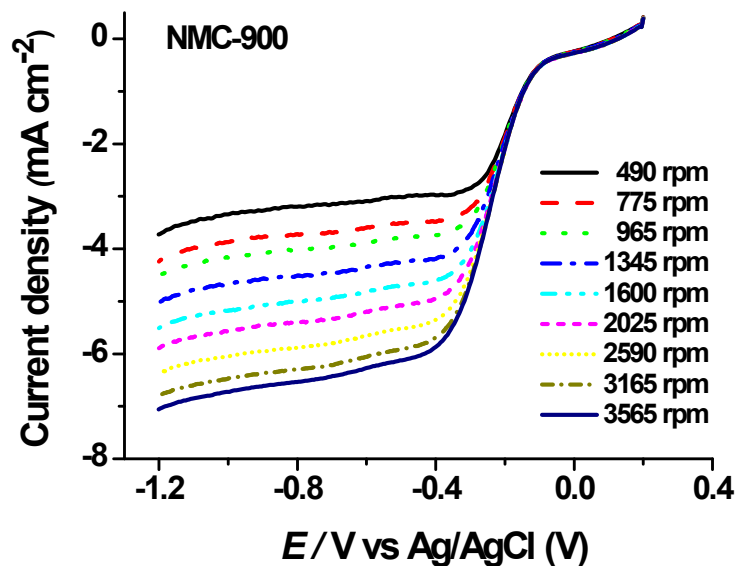


Fig. S5 Rotating disk electrode (RDE) voltammograms of NMC-900 supported GCE in O_2 -saturated 0.1 M KOH solution recorded at a scan rate of 10 $mV\ s^{-1}$ and varied rotation speeds ($490 \sim 3565$ rpm).

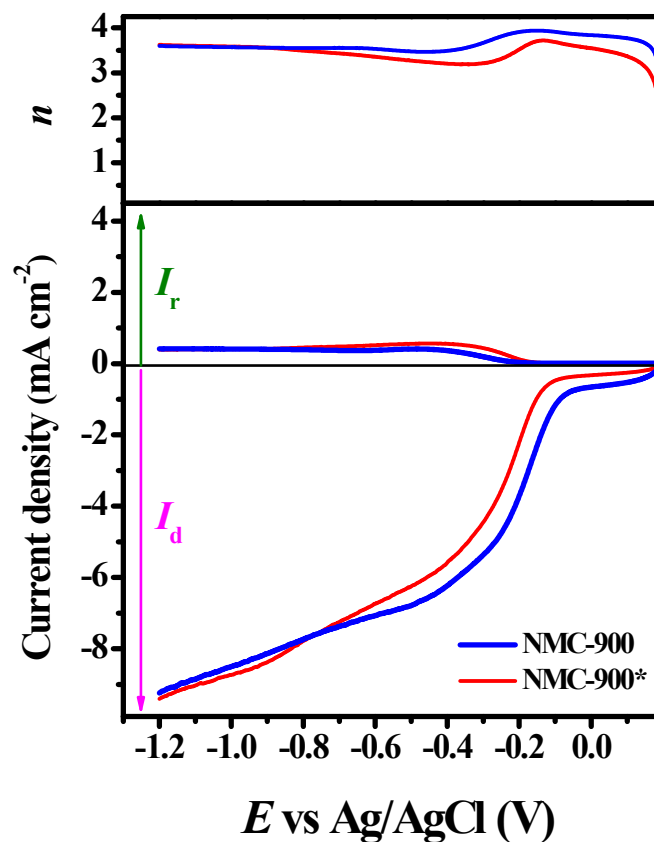


Fig. S6 Bottom: rotating ring-disk electrode (RRDE) of NMC-900 and NMC-900* in O₂-saturated 0.1 M KOH solution. Linear sweep voltammetry (LSV) was performed at a rotating speed of 1,600 rpm with a scanning rate of 50 mV s⁻¹, and the Pt ring electrode was polarized to oxidize the HO₂⁻ intermediates collected from the NMC modified glassy carbon (GC) disk electrode at 0.5 V. That the ring electrode current (I_r) is much less than disk electrode current (I_d), revealing little amount of hydroperoxide ion formation. Top: variations of electron transfer numbers (n) with potential calculated based on RRDE curves. A n value of 3.6 and 3.4 at -0.5 V may be inferred for NMC-900 and NMC-900*, respectively, in good agreement which the average n values calculated based on the rotating disk electrode (RDE) voltammograms (see Table 1).